

## 基于半刚性二羧酸配体的两个三维镉(II)配位聚合物

刘 露<sup>\*,1</sup> 洪梦如<sup>1</sup> 刘莹莹<sup>1</sup> 王智会<sup>1</sup> 李 英<sup>1</sup> 侯红卫<sup>\*,2</sup> 张裕平<sup>1</sup>

(<sup>1</sup> 河南科技学院化学化工学院, 新乡 453003)

(<sup>2</sup> 郑州大学化学与分子工程学院, 郑州 450052)

**摘要:** 通过引入 2 个不同的氮杂环配体, 得到了 2 个 Cd(II) 配位聚合物  $[\text{Cd}(m\text{-phda})(\text{btbb})_{0.5}]_n$  (**1**) 和  $[\text{Cd}(m\text{-phda})(\text{hbmb})_{0.5}]_n$  (**2**) ( $m\text{-H}_2\text{phda}$ =间苯二甲酸), 并对它们的结构进行了表征。结构分析表明配合物 **1** 是一个 6-连接的 *pcu* 拓扑网络, 拓扑符号为  $4^{12}\cdot6^3$ 。配合物 **2** 是一个 5-连接的 *sqp* 拓扑网络, 拓扑符号为  $(4^4\cdot6^6)$ 。另外, 配合物 **1** 和 **2** 表现出较好的热稳定性和不同的荧光行为。

**关键词:** Cd(II); 结构; 拓扑; 荧光

中图分类号: O614.24<sup>2</sup>

文献标识码: A

文章编号: 1001-4861(2018)01-0187-08

DOI: 10.11862/CJIC.2018.006

## Two 3D Cd(II) Coordination Polymers Based on Semi-rigid Dicarboxylic Acid Ligand

LIU Lu<sup>\*,1</sup> HONG Meng-Ru<sup>1</sup> LIU Ying-Ying<sup>1</sup>

WANG Zhi-Hui<sup>1</sup> LI Ying<sup>1</sup> HOU Hong-Wei<sup>\*,2</sup> ZHANG Yu-Ping<sup>1</sup>

(<sup>1</sup>School of Chemistry and Chemical Engineering, Henan Institute of Science and Technology, Xinxian, Henan 453003, China)

(<sup>2</sup>College of Chemistry and Molecular Engineering, Zhengzhou University, Zhengzhou 450052, China)

**Abstract:** Two novel Cd(II) coordination polymers (CPs), formulated as  $[\text{Cd}(m\text{-phda})(\text{btbb})_{0.5}]_n$  (**1**) and  $[\text{Cd}(m\text{-phda})(\text{hbmb})_{0.5}]_n$  (**2**) ( $m\text{-H}_2\text{phda}$ =*m*-phenylenediacetic acid,  $\text{btbb}$ =1,4-bis-(2-(4-thiazolyl)benzimidazole-1-ylmethyl)benzene,  $\text{hbmb}$ =1,1'-(1,6-hexane)bis-(2-methylbenzimidazole)) have been prepared by hydrothermal reactions of the semi-rigid ligand *m*-H<sub>2</sub>phda with Cd(II) ions in the presence of two disparate N-heterocyclic co-ligands and further characterized by infrared spectra (IR), powder X-ray diffraction (PXRD), elemental analyses and thermogravimetric (TG) analyses. **1** possesses a 6-connected 2-fold interpenetrating 3D *pcu* topology net with point symbol of  $4^{12}\cdot6^3$ . **2** exhibits a 5-connected 3D *sqp* network with a Schläfli symbol of  $4^4\cdot6^6$ . Additionally, complexes **1** and **2** present better thermal stabilities, as well as **1** and **2** also show different photoluminescence behaviors in the solid state. CCDC: 988559, **1**; 1524429, **2**.

**Keywords:** Cd(II); structure; topology; fluorescence

Over the past few decades, the metal-organic framework (MOF) materials, by reason of their unique structures, have motivated the chemists to achieve the disparate multifunctional applications in the areas of gas storage and separation<sup>[1-2]</sup>, ion exchange<sup>[3-4]</sup>,

heterogeneous catalysis<sup>[5-6]</sup>, electrical conduction<sup>[7]</sup>, molecular magnets<sup>[8]</sup> and luminescence materials<sup>[9]</sup>. The solvothermal method has been broadly adopted to build MOFs or coordination polymers (CPs), since it not only can ease the matters of ligand solubility, but

收稿日期: 2017-06-15. 收修改稿日期: 2017-09-27.

河南科技学院高层次人才科研启动项目、河南科技学院大学生创新训练计划项目、河南省博士后科研项目、河南省高等学校重点科研项目(No.16A150007)和河南科技学院标志性创新工程项目(No.2015BZ02)资助。

\*通信联系人。E-mail: liululiulu2012@126.com, houthongw@zzu.edu.cn

also can boost the reactivity of the reactant during the crystallization process. Nevertheless, the crystallization process of CPs is influenced by many factors, such as the structural characteristics of ligand, the metal-ligand ratio, the temperature and the solvent systems<sup>[10-11]</sup>, in this method. Among those factors mentioned above, the selection of ligands is of vital importance in the fabrication of CPs. So far, numerous polybasic carboxylic acids ligands have been hired to construct CPs on account of their affluent coordination modes. Here, we choose semi-rigid *m*-phenylenediacetic acid (*m*-H<sub>2</sub>phda) as main ligand. *m*-H<sub>2</sub>phda possesses the following characters: firstly, it possess two carboxylic groups with diversified coordination mode; secondly, the existence of two -CH<sub>2</sub>- groups can make carboxylic groups twist, leading to product unlike conformations. Besides, the synthetic strategy of mixed polycarboxylate and N-donor ligand has been proved to be a fruitful way for the formation of multidimensional structures<sup>[12]</sup>.

Inspired by the above ideas, the reactions of Cd(II) salts and *m*-H<sub>2</sub>phda were executed in the presence of auxiliary ligands 1,4-bis (2-(4-thiazolyl)benzimidazole-1-ylmethyl)benzene (btbb) and 1,1'-(1,6-hexane)bis-(2-methylbenzimidazole) (hbmb) in this essay. Two different three-dimensional (3D) Cd (II) complexes, [Cd (*m*-phda) (btbb)<sub>0.5</sub>]<sub>n</sub> (**1**) and [Cd (*m*-phda) (hbmb)<sub>0.5</sub>]<sub>n</sub> (**2**), have successfully been acquired. And then, the thermal stability and photoluminescence of the complexes **1** and **2** were also reported.

## 1 Experimental

### 1.1 Materials and methods

All reagents and solvents were commercially available without any further purification in addition to ligand btbb and hbmb, which were synthesized according to the literature<sup>[13]</sup>. The data of FT-IR spectra were calendared on a Bruker-ALPHA spectrophotometer with KBr pellets in the scale of 400~4 000 cm<sup>-1</sup>. Elemental analyses (C, H, and N) were carried out on a FLASH EA 1112 elemental analyzer. Powder X-ray diffraction patterns were accomplished on a PANalytical X'Pert PRO diffractometer making use of

Cu Kα<sub>1</sub> radiation (λ=0.154 06 nm) at 40 kV and 40 mA. The XRD patterns were collected in the range of 5°~50°. Thermogravimetric analyses were performed on a Netzsch STA 449C thermal analyzer with a 10 °C · min<sup>-1</sup> heating rate in the air flow. The measurements of the luminescent spectra of the powdered solid samples were conducted on a Hitachi 850 fluorescence spectrophotometer at ambient temperature.

### 1.2 Synthesis of [Cd(*m*-phda)(btbb)<sub>0.5</sub>]<sub>n</sub> (**1**)

A mixture of Cd(NO<sub>3</sub>)<sub>2</sub>·4H<sub>2</sub>O (0.061 7 g, 0.2 mmol), *m*-H<sub>2</sub>phda (0.009 6 g, 0.05 mmol), btbb (0.050 4 g, 0.1 mmol), EtOH (6 mL) and H<sub>2</sub>O (4 mL) was placed in a 25 mL Teflon-lined stainless steel container. The mixture was sealed and heated at 170 °C for three days. After the mixture was cooled to ambient temperature at a rate of 5 °C · h<sup>-1</sup>, yellow block-shaped crystals of **1** were obtained with a yield of 43% (based on Cd). Anal. Calcd. for C<sub>24</sub>H<sub>18</sub>CdN<sub>3</sub>O<sub>4</sub>S(%): C, 51.76; H, 3.25; N, 7.54. Found(%): C, 51.74; H, 3.31; N, 7.58. IR (KBr, cm<sup>-1</sup>): 3 434(m), 2 923(m), 2 854(w), 1 629(m), 1 573(w), 1 475(w), 1 425(s), 1 384(vs), 1 303(w), 927(w), 831(w), 744(w), 657(w), 619(w), 485(w).

### 1.3 Synthesis of [Cd(*m*-phda)(hbmb)<sub>0.5</sub>]<sub>n</sub> (**2**)

A mixture of Cd(Ac)<sub>2</sub>·2H<sub>2</sub>O (0.053 3 g, 0.2 mmol), *m*-H<sub>2</sub>phda (0.009 6 g, 0.05 mmol), hbmb (0.034 6 g, 0.1 mmol), EtOH (5 mL) and H<sub>2</sub>O (5 mL) was placed in a 25 mL Teflon-lined stainless steel container at 160 °C for three days. After the mixture was cooled to room temperature at a rate of 5 °C · h<sup>-1</sup>, yellow block-shaped crystals suitable for X-ray diffraction were obtained with a yield of 55% (based on Cd). Anal. Calcd. for C<sub>21</sub>H<sub>21</sub>CdN<sub>2</sub>O<sub>4</sub>(%): C, 52.78; H, 4.42; N, 5.86. Found(%): C, 52.84; H, 4.46; N, 5.79. IR (KBr, cm<sup>-1</sup>): 3 434(w), 3 052(w), 3 025(w), 2 938(w), 2 917(w), 2 852(w), 1 560(s), 1 475(m), 1 459(m), 1 396(s), 1 292(w), 1 560(s), 1 475(m), 1 459(m), 1 396(s), 1 292(w), 1 272(s), 1 241(w), 1 162(s), 1 089(w), 1 016(m), 941(s), 914(w), 844(w), 798(w), 763(w), 742(m), 727(s), 611(w), 580(w), 437(w).

### 1.4 Crystal structural determination

The collections of crystallographic data of **1** and **2** were fulfilled at room temperature adopting a Rigaku Saturn 724 CCD diffractometer, which was

equipped with Mo  $K\alpha$  radiation ( $\lambda=0.071\ 073\ \text{nm}$ ). Crystal size of **1** is  $0.20\ \text{mm} \times 0.19\ \text{mm} \times 0.15\ \text{mm}$ . Crystal size of **2** is  $0.21\ \text{mm} \times 0.19\ \text{mm} \times 0.17\ \text{mm}$ . Absorption corrections were enforced via utilizing multi-scan program. The data were corrected on the basis of Lorentz and polarization effects. The structures were handled by firsthand methods and then refined by means of  $F^2$  with a full-matrix least-squares technique that adopted the SHELXL-97 crystallographic

software package<sup>[14]</sup>. All of the non-hydrogen atoms were refined anisotropically. The hydrogen atoms of ligands were assigned at perfect positions capitalizing on a riding model and then refined isotropically. Crystallographic data and structure refinement details for **1** and **2** are generalized in Table 1. Selected bond lengths and bond angles of **1** and **2** are listed in Table 2.

CCDC: 988559, **1**; 1524429, **2**.

**Table 1** Crystal data and structure refinement details for complexes **1** and **2**

Complex	<b>1</b>	<b>2</b>
Formula	$\text{C}_{24}\text{H}_{18}\text{CdN}_3\text{O}_4\text{S}$	$\text{C}_{21}\text{H}_{21}\text{CdN}_2\text{O}_4$
Formula weight	556.87	477.80
Temperature / K	293(2)	293(2)
Crystal system	Triclinic	Monoclinic
Space group	$C2/c$	$P2_1/c$
$a / \text{nm}$	1.674 3(3)	1.158 7(2)
$b / \text{nm}$	1.996 1(4)	1.980 3(4)
$c / \text{nm}$	1.460 8(3)	0.872 65(17)
$\beta / (^\circ)$	93.23(3)	105.02(3)
$V / \text{nm}^3$	4.874 0(17)	1.934 0(7)
$Z$	8	4
$D_c / (\text{g} \cdot \text{cm}^{-3})$	1.518	1.641
$\mu / \text{mm}^{-1}$	1.016	1.159
$F(000)$	2 232	964
GOF on $F^2$	1.100	0.962
$R_1 [I > 2\sigma(I)]^a$	0.092 2	0.031 4
$wR_2$ (all data) <sup>b</sup>	0.240 5	0.071 7

$$^a R_1 = \sum ||F_o| - |F_c|| / \sum |F_o|; ^b wR_2 = [\sum w(F_o^2 - F_c^2)^2 / \sum w(F_o^2)]^{1/2}.$$

**Table 2** Selected bond lengths (nm) and bond angles ( $^\circ$ ) for **1** and **2**

Complex <b>1</b>					
Cd(1)-O(1)#1	0.223 7(7)	Cd(1)-O(2)	0.230 6(7)	Cd(1)-O(3)#2	0.236 5(9)
Cd(1)-O(4)#2	0.229 3(8)	Cd(1)-N(1)	0.261 4(10)	Cd(1)-N(2)	0.229 5(9)
O(1)#1-Cd(1)-N(2)	92.6(3)	O(1)#1-Cd(1)-O(4)#2	92.2(3)	N(2)-Cd(1)-O(4)#2	148.9(4)
O(1)#1-Cd(1)-O(2)	108.8(3)	N(2)-Cd(1)-O(2)	86.0(3)	O(4)#2-Cd(1)-O(2)	121.2(3)
O(1)#1-Cd(1)-O(3)#2	149.1(3)	N(2)-Cd(1)-O(3)#2	115.6(4)	O(4)#2-Cd(1)-O(3)#2	57.2(3)
O(2)-Cd(1)-O(3)#2	86.6(3)	O(1)#1-Cd(1)-N(1)	102.5(3)	N(2)-Cd(1)-N(1)	67.4(4)
O(4)#2-Cd(1)-N(1)	81.5(3)	O(2)-Cd(1)-N(1)	139.7(3)	O(3)#2-Cd(1)-N(1)	79.0(3)
Complex <b>2</b>					
Cd(1)-N(1)	0.223 5(3)	Cd(1)-O(2)	0.225 7(3)	Cd(1)-O(4)#1	0.227 8(2)
Cd(1)-O(3)	0.235 0(2)	Cd(1)-O(1)	0.236 3(3)	Cd(1)-O(3)#1	0.248 8(2)
N(1)-Cd(1)-O(2)	144.37(10)	N(1)-Cd(1)-O(4)#1	104.29(9)	O(2)-Cd(1)-O(4)#1	111.18(10)
N(1)-Cd(1)-O(3)	91.63(8)	O(2)-Cd(1)-O(3)	89.20(12)	O(4)#1-Cd(1)-O(3)	83.34(8)

Continued Table 2

N(1)-Cd(1)-O(1)	91.88(9)	O(2)-Cd(1)-O(1)	54.56(10)	O(4)#1-Cd(1)-O(1)	159.57(10)
O(3)-Cd(1)-O(1)	108.99(11)	N(1)-Cd(1)-O(3)#1	105.80(8)	O(2)-Cd(1)-O(3)#1	97.62(12)
O(4)#1-Cd(1)-O(3)#1	54.32(8)	O(3)-Cd(1)-O(3)#1	136.75(7)	O(1)-Cd(1)-O(3)#1	109.61(11)

Symmetry codes: #1:  $-x+1/2, -y+1/2, -z+1$ ; #2:  $-x+1/2, y+1/2, -z+3/2$  for **1**; #1:  $x, -y+1/2, z+1/2$  for **2**.

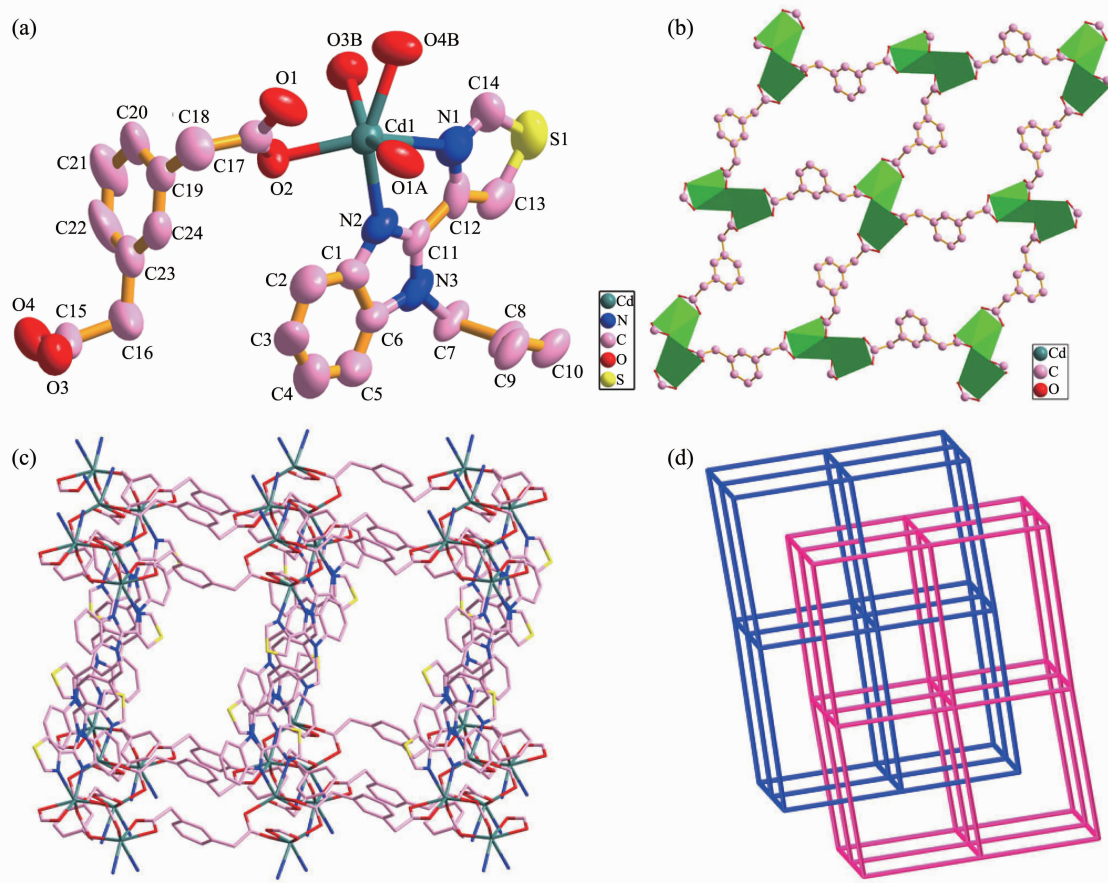
## 2 Results and discussion

### 2.1 Structure description of $[\text{Cd}(m\text{-phda})(\text{btbb})_{0.5}]_n$ (**1**)

The results of crystallographic analysis reveal that **1** crystallizes in monoclinic system with  $C2/c$  space group. The asymmetric unit of complex **1** consists of one Cd(II) ion, half btbb ligand and one  $m\text{-phda}^{2-}$  ligand. As shown in Fig.1a, each Cd(II) ion is in the distorted octahedral geometry with  $\text{CdO}_4\text{N}_2$  coordination environment finished by two nitrogen atoms (N1 and N2) from one btbb ligand and four oxygen atoms

(O1A, O2, O3B, O4B) from three different  $m\text{-phda}^{2-}$  ligands. The distances of Cd-O/N bonds range from 0.223 7 (7) to 0.261 4 (10) nm, which are similar to other Cd-based complexes<sup>[15]</sup>.

The btbb ligand adopts asymmetric *trans*-conformation with  $\text{N}_{\text{donor}} \cdots \text{N}-\text{C}_{\text{sp}^3} \cdots \text{C}_{\text{sp}^3}$  torsion angles of  $69.578^\circ$ . Ligand  $m\text{-phda}^{2-}$  also adopts asymmetric *trans*-conformation, and the angles of two  $-\text{CH}_2-$  are  $114.255^\circ$  and  $111.979^\circ$ . The two carboxylate groups of the  $m\text{-phda}^{2-}$  ligand show different coordination modes: one carboxylate group adopts bidentate chelating mode and the other adopts bidentate bridging mode.



Ellipsoid probability level in (a): 50%; Symmetry codes: #1:  $-x+1/2, -y+1/2, -z+1$ ; #2:  $-x+1/2, y+1/2, -z+3/2$

Fig.1 (a) Coordination environment of Cd(II) ion with hydrogen atoms omitted for clarity; (b) Two-dimensional (2D) sheet generated by Cd(II) ions and  $m\text{-phda}^{2-}$  linkers in **1**; (c) Schematic view of the 3D framework built by 2D  $\text{Cd(II)}/m\text{-phda}^{2-}$  layers and btbb pillars in **1**; (d) Schematic representation of the 2-fold interpenetrated topology nets for **1**

Each  $m\text{-phda}^{2-}$  anion links three  $\text{Cd(II)}$  ions resulting in a 2D sheet structure parallel to the  $bc$  plane (Fig. 1b). The architecture of the 2D sheet is composed of the dinuclear unit  $[\text{Cd}_2(\text{COO})_2]$  with  $\text{Cd}\cdots\text{Cd}$  distance of 0.392 06 nm. The dinuclear units are further pillared upward and downward by two *trans*-conformational btbb ligands into a 3D pillar-layered framework (Fig. 1c).

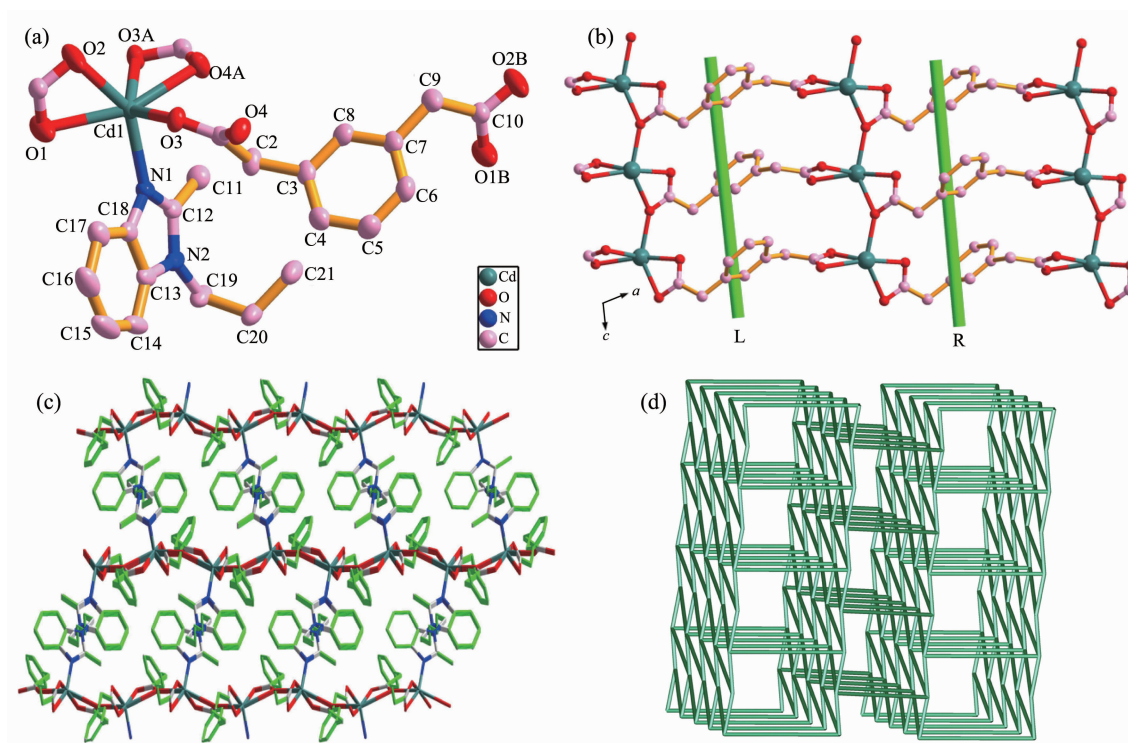
Better insight into the present 3D framework can be accessed by the topological method. If the dinuclear unit  $[\text{Cd}_2(\text{COO})_2]$  is viewed as a 6-connected node, and the btbb and  $m\text{-phda}^{2-}$  serves as linkers, the 3D structure can be classified as a 6-connected  $pcu$  topology with point symbol of  $4^{12}\cdot6^3$  (Fig. 1d). The void space in the single framework is so large that two identical 3D frameworks interpenetrate each other to form a 2-fold interpenetrating architecture (Fig. 1d).

## 2.2 Structure description of $[\text{Cd}(m\text{-phda})(\text{hbmb})_{0.5}]_n$ (**2**)

The single crystal X-ray diffraction analysis for **2**

shows that **2** crystallizes in monoclinic system with  $P2_1/c$  space group. The asymmetric unit of complex **2** consists of one  $\text{Cd(II)}$  ion, one  $m\text{-phda}^{2-}$  ligand, half hbmb ligand. As depicted in Fig. 2a, each  $\text{Cd(II)}$  ion is six-coordinated by five carboxylate oxygen atoms (O1, O2, O3, O3A and O4A) from three  $m\text{-phda}^{2-}$  anions and one nitrogen atom (N1) from one hbmb ligand. The  $\text{Cd-O}$  bond distances vary from 0.225 7(3) to 0.248 8(2) nm, while the  $\text{Cd-N1}$  bond length is 0.223 5(3) nm. The  $m\text{-phda}^{2-}$  anions adopt asymmetric *trans*-conformation, and the angles of two  $-\text{CH}_2-$  are  $113.385^\circ$  and  $115.813^\circ$ . Ligand hbmb adopts symmetric *trans*-conformation with an  $\text{N}_{\text{donor}}\cdots\text{N}-\text{C}_{\text{sp}^3}\cdots\text{C}_{\text{sp}^3}$  torsion angle of  $97.555^\circ$ .

In **2**, the ligand  $m\text{-phda}^{2-}$  adopts  $(\kappa^2-\kappa^1-\mu_2)-(\kappa^2)-\mu_3$  coordination information. The  $\text{Cd(II)}$  ions are connected by  $m\text{-phda}^{2-}$  anions to form a 2D sheet structure with alternately arranged left- and right-handed helical chains (Fig. 2b). Both the helical pitches are 0.872 65(17) nm corresponding to the length of  $c$ -axis.



Ellipsoid probability level in (a): 50%; Symmetry codes: #1:  $x, 1/2-y, 1/2+z$ ; #2:  $1+x, y, z$

Fig. 2 (a) Coordination environment of  $\text{Cd(II)}$  ion with hydrogen atoms omitted for clarity; (b) View of the 2D sheet structure with alternately arranged left- and right-handed helical chains parallel to the  $ac$  plane; (c) Schematic view of the 3D framework built by 2D  $\text{Cd(II)}/m\text{-phda}^{2-}$  layers and hbmb pillars in **2**; (d) Schematic view of the 3D topology network with a vertex symbol of  $4^4\cdot6^6$  for **2**



Then the 2D nets are connected by hbmb ligands in a *trans*-conformation via the Cd-N connections to product a 3D pillar-layered framework (Fig.2c). The topological analysis is performed on **2** (Fig.2d). We can consider each  $[\text{CdCO}_3]$  unit as a 5-connecting node, which is linked to two  $[\text{CdCO}_3]$  units by two *m*-phda<sup>2-</sup> ligands and one hbmb ligand. The *m*-phda<sup>2-</sup> and hbmb can be defined as linkers, the 3D framework of **2** can be described as a 5-connected *sqp* topology net with point symbol of  $4^4 \cdot 6^6$  (Fig.2d).

### 2.3 Effects of the coordination modes of the *m*-phda<sup>2-</sup> anion and N-donor co-ligands on the structures of complexes **1** and **2**

As described above, the semi-rigid *m*-phda<sup>2-</sup> ligand presents asymmetric *trans*-conformation in **1** and **2**. The free conformations of  $-\text{CH}_2-$  spacer vastly enrich the structures of **1** and **2**. Although the *m*-phda<sup>2-</sup> ligand all acts as a three-connector to link three Cd(II) ions in **1** and **2**, their coordination modes are different. For **1**, the angles of two  $-\text{CH}_2-$  are  $114.255^\circ$  and  $111.979^\circ$ , singly. The ligand *m*-phda<sup>2-</sup> adopts  $(\kappa^1-\kappa^1)-(\kappa^2)-\mu_3$  coordination information, in which two carboxyl groups adopt *syn-anti*- $\mu_2-\eta^1:\eta^1$  and  $\mu_1-\eta^1:\eta^1$  coordination modes, severally. This kind of *m*-phda<sup>2-</sup> anion links three Cd(II) ions forming an ordinary 2D net. For **2**, the angles of two  $-\text{CH}_2-$  are  $113.385^\circ$  and  $115.813^\circ$ , respectively. The ligand *m*-phda<sup>2-</sup> adopts  $(\kappa^2-\kappa^1-\mu_2)-(\kappa^2)-\mu_3$  coordination information, in which two carboxylic groups act as  $\mu_2-\eta^2:\eta^1$  and  $\mu_1-\eta^1:\eta^1$  modes, singly. This type of *m*-phda<sup>2-</sup> anion connects three Cd(II) ions building a 2D net with alternately arranged left- and right-handed helical chains.

The introduction of N-donor ligands into Cd(II)/*m*-phda<sup>2-</sup> system will make the structure of complexes more complicated and more beautiful. In **1**, btbb adopts asymmetric *trans*-conformation with  $\text{N}_{\text{donor}} \cdots \text{N}-\text{C}_{\text{sp}^3} \cdots \text{C}_{\text{sp}^3}$  torsion angles of  $69.578^\circ$ . btbb acts as pillars linking the adjacent Cd(II)/*m*-phda<sup>2-</sup> nets into a 2-fold interpenetrating *pcu* 3D framework with point symbol of  $4^{12} \cdot 6^3$ . In **2**, hbmb adopts symmetric *trans*-conformation with an  $\text{N}_{\text{donor}} \cdots \text{N}-\text{C}_{\text{sp}^3} \cdots \text{C}_{\text{sp}^3}$  torsion angle of  $97.555^\circ$ . Hbmb serves as pillars connecting the neighboring Cd(II)/*m*-phda<sup>2-</sup> nets into a *sqp* 3D framework with point symbol of  $4^4 \cdot 6^6$ .

### 2.4 XRD patterns and thermal analyses

The PXRD patterns of complexes **1** and **2** are shown in Fig.3. The PXRD patterns of the two complexes determined by experiment are in line with the simulated ones of single crystals, which indicate that each of the two complexes is pure phase. To assess the stability of the coordination architectures, thermogravimetric analyses (TGA) of **1** and **2** were carried out (Fig.4). For **1**, the weight loss from 336 to

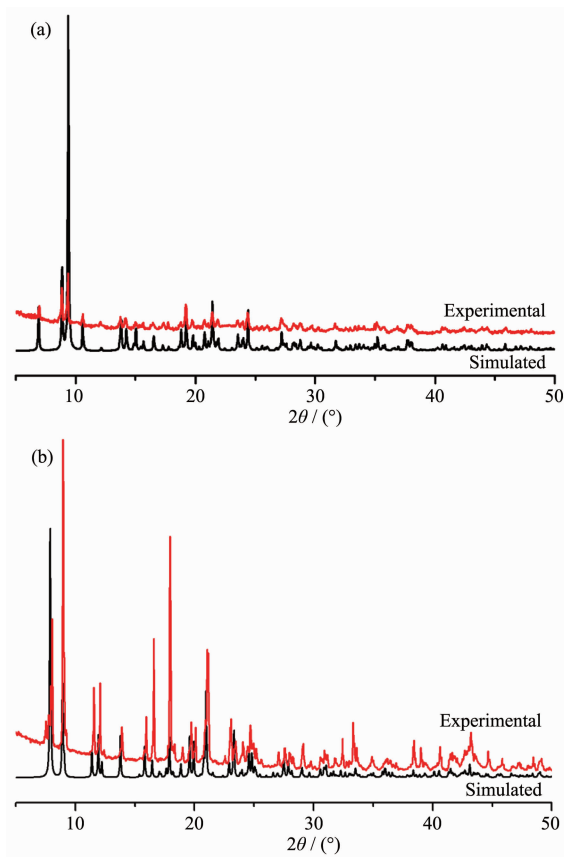


Fig.3 Experimental (top) and simulated (bottom) PXRD patterns of complexes **1** (a) and **2** (b)

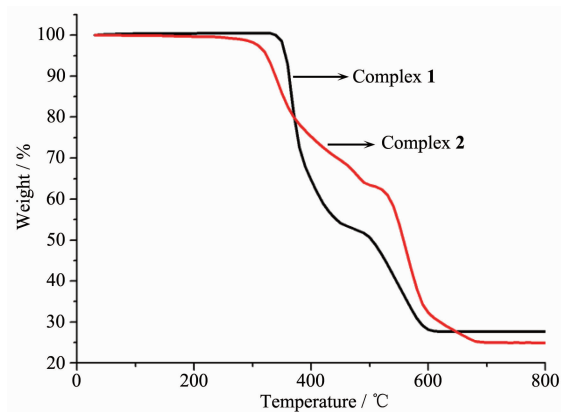


Fig.4 TGA curves of complexes **1** and **2**

607 °C corresponds to the decomposition of half btbb ligand and one *m*-phda<sup>2-</sup> ligand. A residue of CdO (Obsd. 27.69%, Calcd. 26.87%) is discovered. As for complex **2**, the weight loss in the range of 302~676 °C represents the decomposition of the whole framework. A residue of CdO (Obsd. 24.23%, Calcd. 23.06%) is discovered.

## 2.5 Photoluminescence properties

The solid-state luminescence spectra of complexes **1** and **2**, the free ligand *m*-H<sub>2</sub>phda and the relevant auxiliary ligands were investigated at room temperature (Fig.5). The spectrum of *m*-H<sub>2</sub>phda and btbb shows one strong emission at 387 nm ( $\lambda_{\text{ex}}$ =330 nm) and 399 nm ( $\lambda_{\text{ex}}$ =385 nm), respectively, and the

spectrum of hbmb shows one weaker emission at 306 nm ( $\lambda_{\text{ex}}$ =275 nm). For complex **1**, excited at 335 nm, it gives rise to an emission band at 391 nm. As compared to the btbb ligand, a little hypsochromic shift (8 nm) is observed. As compared to the *m*-H<sub>2</sub>phda ligand, a little red shift (4 nm) is observed. For complex **2**, the emission spectrum displays a emission band centered at 384 nm with excitation maximum at 337 nm and the emission band presents little hypsochromic shift (3 nm) compared with that of the ligand *m*-H<sub>2</sub>phda. Obviously, the emission spectra of **1** can be mainly ascribed to the intraligand emission of *m*-phda<sup>2-</sup> and btbb, while that of **2** can be mainly attributed to the intraligand emission of *m*-phda<sup>2-</sup> and hbmb.

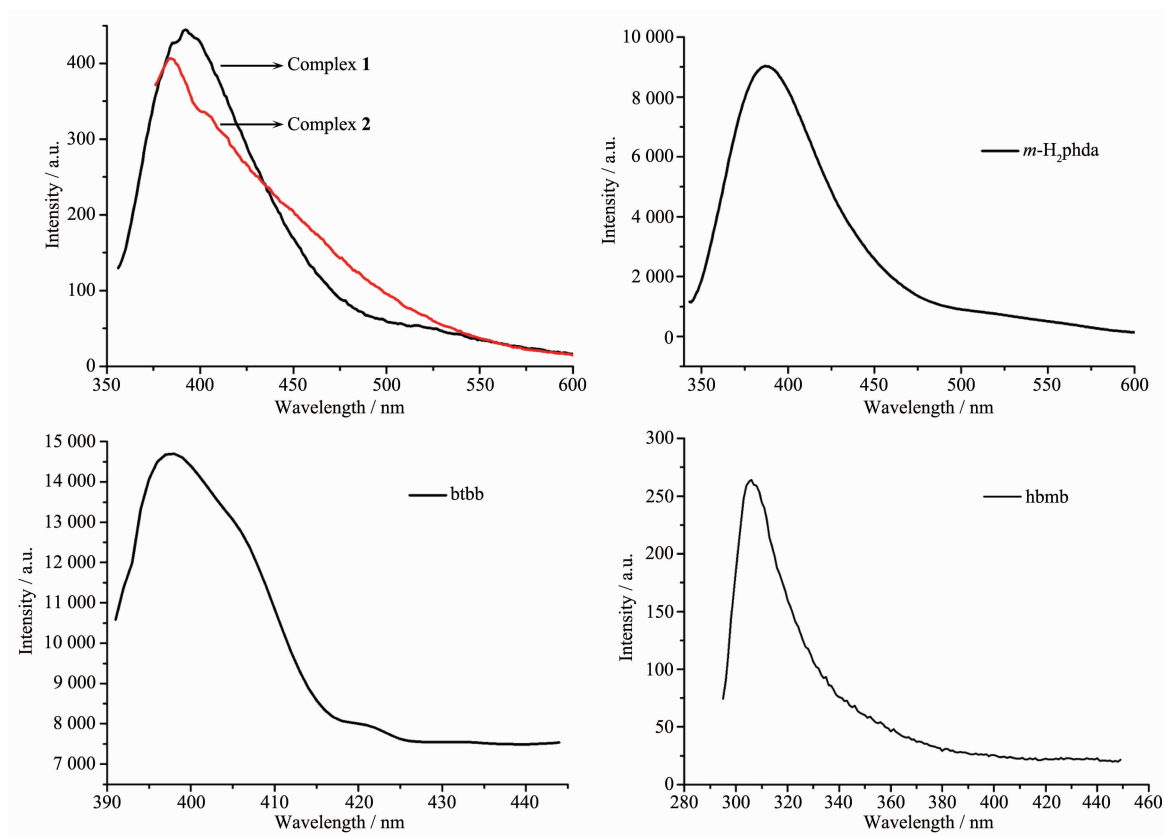


Fig.5 Solid-state photoluminescent spectra of complexes **1** and **2** and free ligand *m*-H<sub>2</sub>phda, btbb, hbmb

## 3 Conclusions

In a nutshell, the synchronous use of the *m*-H<sub>2</sub>phda ligand and related N-donor co-ligands to react with Cd(II) ions affords two CPs. These two complexes present enthralling structural motifs. This work

manifests that the hire of mixed-ligands is a feasible strategy to adjust and control the formation of high-dimensionality frameworks. The structural multiformity of **1** and **2** also imply that the conformation of the *m*-phda<sup>2-</sup> ligand and additional N-donors play pivotal roles in the assembly of the final skeleton.

## References:

- [1] Sumida K, Rogow D L, Mason J A, et al. *Chem. Rev.*, **2012**, **112**:724-781
- [2] Qin L, Ju Z M, Wang Z J, et al. *Cryst. Growth Des.*, **2014**, **14**:2742-2746
- [3] Yao R X, Xu X, Zhang X M. *Chem. Mater.*, **2012**, **24**:303-310
- [4] Dalrymple S A, Shimizu G K H. *Chem. Eur. J.*, **2002**, **8**:3010-3015
- [5] Huang S L, Jia A Q, Jin G X. *Chem. Commun.*, **2013**, **49**:2403-2405
- [6] Huang S L, Weng L H, Jin G X. *Dalton Trans.*, **2012**, **41**:11657-11662
- [7] Gándara F, Uribe-Romo F J, Britt D K, et al. *Chem. Eur. J.*, **2012**, **18**:10595-10601
- [8] Whlert S, Wriedt M, Fic T, et al. *Inorg. Chem.*, **2013**, **52**:1061-1068
- [9] Cui Y J, Yue Y F, Qian G D, et al. *Chem. Rev.*, **2012**, **112**:1126-1162
- [10] Tong M L, Ye B H, Cai J W, et al. *Inorg. Chem.*, **1998**, **37**:2645-2650
- [11] Zhang W L, Liu Y Y, Ma J F, et al. *Cryst. Growth Des.*, **2008**, **8**:1250-1256
- [12] Liu L, Lyu X F, Zhang L, et al. *CrystEngComm*, **2014**, **16**:8736-8746
- [13] Bronisz R. *Inorg. Chem.*, **2005**, **44**:4463-4465
- [14] Sheldrick G M. *Acta Crystallogr. Sect. A: Found. Crystallogr.*, **2008**, **A64**:112-122
- [15] Shi X J, Wang X, Li L K, et al. *Cryst. Growth Des.*, **2010**, **10**:2490-2500